Acta Universitatis Sapientiae
Electrical and Mechanical Engineering, 10 (2018) 42-66

DOI: 10.2478/auseme-2018-0003

GA/PSO Robust Sliding Mode Control of Aerodynamics in Gas Turbine

Abdesselam DEBBAH[1], Hamid KHERFANE[2]

[1] L2RCS Laboratory, Department of Electronics, Badji Mokhtar University, Annaba, Algeria, Department of Petro-chemical and Process Engineering, 20 Aout 1955 University, Skikda, Algeria, e-mail: debbeha@yahoo.fr
[2] L2RCS Laboratory, Department of Electronics, Badji Mokhtar University, Annaba, Algeria
e-mail: hamid_kherfane@yahoo.fr

Manuscript received September 15, 2018; revised December 15, 2018.

Abstract: In gas turbine process, the axial compressor is subjected to aerodynamic instabilities because of rotating stall and surge associated with bifurcation nonlinear behaviour. This paper presents a Genetic Algorithm and Particle Swarm Optimization (GA/PSO) of robust sliding mode controller in order to deal with this transaction between compressor characteristics, uncertainties and bifurcation behaviour. Firstly, robust theory based equivalent sliding mode control is developed via linear matrix inequality approach to achieve a robust sliding surface, then the GA/PSO optimization is introduced to find the optimal switching controller parameters with the aim of driving the variable speed axial compressor (VSAC) to the optimal operating point with minimum control effort. Since the impossibility of finding the model uncertainties and system characteristics, the adaptive design widely considered to be the most used strategy to deal with these problems. Simulation tests were conducted to confirm the effectiveness of the proposed controllers.

Keywords: aerodynamic instabilities, variable speed axial compressor (VSAC), sliding mode control (SMC), adaptive robust control, genetic algorithm (GA), particle swarm optimization (PSO).

1. Introduction

The increased performances are potentially achievable with modern gas turbines operating close to the maximum pressure rise, and under physical constraints [1]. This characteristic makes it very required in critical industries such as jet-engine, power generation and petrochemical. The gas turbine is however subjected to nonlinear phenomena of different nature: aerodynamic (pumping and rotating stall), aero-elasticity (the float) and combustion, that do not allow proper operation [2]. The gas turbine suffers from two types of aerodynamic instabilities, namely rotating stall and surge, which are closely related to the limitations of their efficiency and performance [2]. Rotating stall is a non-axisymmetric perturbation that travels around the annulus of the axial compressor while surge is a large axial oscillation of flow [2].

In 1997, Gravdahl and Egeland developed a model and investigated surge and speed control. For the first time, the model developed by Gravdahl for axial compressors considered the B-parameter (proportional to the speed of the compressor) as a state and included higher harmonics of rotating stall as well [3]. Contrary to Gravdahl's variable speed model, the Moore-Greitzer original model does not imply any rotating stall development, since the working point is situated at an adequate margin from the surge line [4]. This temporary stall development and pressure drop can cause trouble for the normal turbo machines' operation. Furthermore, including model uncertainties (the precise estimation of model parameters, especially in the unstable area, being difficult) and external perturbations make the problem even more challenging [3], [4]. Finally, the squared amplitude of stall modes used as state variables are experimentally difficult to measure and full-state feedback cannot be considered in control design. In order to overcome this issue, throttle valve and Close-Coupled Valve (CCV) actuation are used to guarantee the stability, and a drive torque is applied to increase the speed of the rotor. The CCV is considered to be one of the most promising actuation methods [5]. The investigation on the model dynamics makes the Robust Sliding Mode controller (RSMC) the favorite control strategy. It is well known for its high accuracy, fast dynamic response, stability, the simplicity of implementation, and robustness for changes in uncertainties and external disturbances for dynamic systems [6]. But in real conditions, the prior knowledge on the upper bound of the disturbances and the high frequency switching known as chattering will reduce the system's robustness, and can excite unwanted dynamics that risk to damage or even destroy the system studied [6]. Also, the matched condition and affine form of the control law can't be guaranteed for all steady states especially for highly uncertain, nonlinear and complex systems. Adaptive control law could lead to a stable closed-loop system and the deviation from the sliding surface is bounded [7].

Motivation of this work comes from the fact that other past-proposed controllers usually devoted efforts on stabilizing axial compressors are based on the constant speed assumption, and even if the reported achievements [6], [7], [8], [9], [10], [11], [12], [13] investigate the variable speed model in close loop control, they propose some conservative assumptions that make the controller efficient in a very restricted operating range, as reported in [2], [5], [14]. The Gravdahl-England based models are used in order to design such controllers; however, they are idealized models for variable speed axial compressor (VSAC) systems. Therefore, they never represent the nature perfectly. From the other point of view, in real conditions, the prior knowledge of disturbance and uncertainty becomes difficult. Thus, designing a control system in which information about disturbance, uncertainty, and dynamics of the system is used cannot be satisfactory for real applications. To accomplish the mentioned motivation, a Linear Matrix Inequality (LMI) optimization is used to design the equivalent control to guarantee the asymptotic stability regarding the speed transition behaviour, and GA/PSO optimized switching control is developed to tackle the system uncertainties, perturbations, and high-frequency behaviour of the controller with an efficient and effective constraint-handling. The proposed intelligent control system is developed and utilized to control rotating stall, surge and speed in axial compressors, without the need of prior knowledge on system uncertainties and perturbations. The outline of this paper is as follows. The variable speed axial compressor is presented in Section 2. Section 3 shows robust approach design. Section 4 describes the genetic algorithm and particle swarm optimization adaptive base on robust SMC. Section 5 shows the simulations results. Section 6 concludes with a summary and discussion.

2. The model

The compression process studied in this paper involves an intake duct, inlet guide vanes IGV, a variable speed axial compressor, the exit duct, plenum volume (turbine), varying area throttle valve, varying area close-coupled valve (*Fig. 1*). The throttle can be viewed as a streamlined model of a turbine [2].

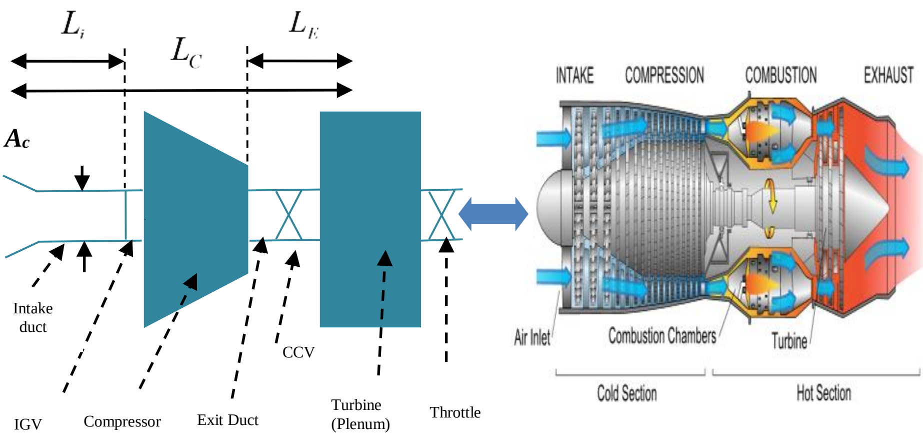

Figure 1: Schematic of the system showing non-dimensional lengths [2].

Gravdahl developed a model for the axial compressor, the exit duct, plenum volume (turbine), varying area throttle valve, varying area close-coupled valve

(*Fig. 1*). The throttle can be viewed as a streamlined model of a turbine [2]. Gravdahl developed a model for variable speed axial compressors and considered the speed of the rotor as a state variable [2]. Later, Zaiet et al. [8] modified the model to include the pressure drop over a CCV and to make it suitable for control applications. The states ϕ, ψ and U denote respectively the annulus averaged mass flow coefficient, the non-dimensional plenum pressure, and the speed of the rotor (m/s). $t = \frac{U_d \cdot t_d}{R}$ is a non-dimensional time, where t_d is the dimensional time, R is the mean compressor radius, and U_d is the desired speed. J_1 is the squared amplitude of the first harmonic of the rotating stall [5]. The actuators' forces are input variables u_1, u_2 and u_3 defined respectively as: the pressure drop over CCV, the throttle gain, and the non-dimensional drive torque being used to increase the speed. At an operating point ($\Phi_0=0.55$, $\Psi_0=0.66$, $U_0=9.617$), the dynamic model can be given in the form of state-space equations in error coordinates (see [1], [2] for more details). The model which only includes the first harmonic of the rotating stall and comprises actuator forces is given in the following equations:

$$\begin{aligned}\frac{d\phi(t)}{dt} = \frac{H}{l_c(t)}\Bigg[&-\frac{\psi(\mathrm{t})+\Psi_0-\psi_{c0}}{H}+1+\frac{3}{2}\left(\frac{\phi(t)+\Phi_0}{W}-1\right)\left(1-\frac{J_1(t)}{2}\right)\\ &-\frac{1}{2}\left(\frac{\phi(t)+\Phi_0}{W}-1\right)^3-\frac{u_1(t)}{H}-C_1J_1(t)\\ &-G_1(\phi(t)+\Phi_0)u_3+G_1c(\phi(t)+\Phi_0)^3+\Delta_\psi(t)\Bigg]\end{aligned} \tag{1}$$

$$\begin{aligned}\frac{dJ_1(t)}{dt} = J_1(t)\Bigg[&1-\left(\frac{\phi(t)+\Phi_0}{W}-1\right)^2-\frac{J_1(t)}{4}-G_2-G_3u_3(t)\\ &+G_3c(\phi(t)+\Phi_0)^2-\frac{1}{\gamma_v^2}C_2(\phi(t)+\Phi_0)\Bigg]\frac{3aH}{(1-m_U(t)a)W}\end{aligned} \tag{2}$$

$$\begin{aligned}\frac{d\psi(\mathrm{t})}{d\zeta} = \frac{\Lambda_2}{U(t)+U_0}&\left(\phi(t)+\Phi_0-u_2(t)\sqrt{\psi(t)}\right)\\ &-2\Lambda_1\frac{U(t)+U_0}{b}\,(\psi(t)+\Psi_0)u_3(t)\\ &+2\Lambda_1\frac{U(t)+U_0}{b}\,(\psi(t)+\Psi_0)c(\phi(t)+\Phi_0)^2-\Delta_\phi(t)\end{aligned} \tag{3}$$

$$\frac{dU(t)}{d\zeta} = \Lambda_1(U(t)+U_0)^2u_3(t) - \Lambda_1(U(t)+U_0)^2c(\phi(t)+\Phi_0)^2 \qquad (4)$$

In the above equations:

$$I_c(t) = l_i + l_E\frac{U_d}{U(t)} + \frac{1}{a},\ m_u(t) = (1-m)\frac{U_d}{U(t)} - 1,\ C_1 = \frac{W^2}{2H\gamma_v^2},$$
$$C_2 = \frac{4W}{3H},\ G_1 = \frac{U_0\Lambda_1 l_E}{bH},\ G_2 = \frac{\mu W}{3aH},\ G_3 = \frac{2U_0\Lambda_1(m-1)W}{3Hb} \qquad (5)$$

The definition of the remaining model parameters *H, W,* ψ_{c0}, γ_v , $\Lambda_1, \Lambda_2, m,$ $b,\ \mu,\ a,\ \rho_1 \cong \frac{1}{l_c(t)},\ \rho_2 \cong \frac{3aH}{(1-m_U(t)a)W}$ which are all positive non-zero parameters, can be found in [4], [5]. To investigate the effect of the uncertainties, we introduce Δ_Ψ and Δ_Φ in the model. Δ_Φ consists of two terms: $\Phi_d(t)$ is a time varying mass flow disturbance and introduces a constant or slow varying uncertainty in the throttle characteristic. Similarly, Δ_Ψ consists of two terms: $\Psi_d(t)$ is a time varying pressure disturbance and d_Ψ can be considered as a constant or slow varying uncertainty in the compressor map. Furthermore, it is supposed that these uncertain terms are bounded.

3. Robust design approach

Let us consider the model (1, 2, 3, 4) with (5) as a MIMO norm bounded form [15-20]:

$$\dot{\underline{x}}(t) = (\boldsymbol{A} + \Delta\boldsymbol{A}(t))\cdot \underline{x}(t) + \boldsymbol{B}\cdot(\underline{u}(t) + \underline{\Delta_x}(t))$$
$$\underline{y}(t) = \boldsymbol{C}\cdot \underline{x}(t) \qquad (6)$$

From the state variables $x=(J_1,\phi,\psi,U) \in R^4$ taking $y=(\phi,\psi,U) \in R^3$ as a smooth measurable output vector. In spite of the fact that J_1 is the fourth state variable, it cannot be measured; moreover its nature as a perturbation conveys the idea that it can be considered as an uncertain term. This approach simplifies the control design and makes the proposed control method pertinent [4]. In (6), *A* and *B* are respectively the state and control matrix of the system at the operating point considered the origin (ϕ_0, ψ_0, U_0) [18-20]. Here, $\Delta A(t) = f_1(\phi_0,\psi_0,U)$ is the uncertainty in the dynamic matrix corresponding to the variable speed behavior, $\Delta_x(t) = f_2(J_1,\phi,\psi,U)$ are the model uncertainties, external disturbance and perturbations with unknown bound. Our objective is to stabilize the efficient operating point *($J_1=0$, $\phi=0.5$, $\psi=0.66$)* for two different speeds, low speed *($U_d=40$ m/s)* and high speed *($U_d=150$ m/s).*

Assumption 1: $f_1(\phi,\psi,U)$ and $f_2(J_1,\phi,\psi,U)$ are continuous and bounded polynomial functions of uncertainties, disturbances and J_1. Due to the boundedness of J_1, ϕ and U assumption 1 is satisfied as reported in [2], [5].

A. Reformulating the problem to equivalent sliding mode control

Consider the following linear continuous sliding function [15]:

$$\underline{\sigma_x}(t) = \boldsymbol{S}\cdot \underline{x}(t) = \boldsymbol{B}^T \cdot \boldsymbol{P}\cdot \underline{x}(t) \tag{7}$$

where $\boldsymbol{S} \in R^{3x3}$ and $\boldsymbol{P} \in R^{3x3}$ is symmetric positive definite matrix. From (6) and (7), the equivalent control law may be obtained as:

$$\underline{u_{eq}}(t) = -(\boldsymbol{S}\cdot\boldsymbol{B})^{-1}\cdot \boldsymbol{S}\cdot\boldsymbol{A}\cdot \underline{x}(t) \tag{8}$$

with $\boldsymbol{S} = \boldsymbol{B}^T \cdot \boldsymbol{P}$ and $\boldsymbol{S}\cdot\boldsymbol{B}$ is non-singular. It should be remarked that the obtained control law contains some uncertain terms, which can be deduced from the non-linear system. The non-linear part of controller called switching control, will be taken as [15]:

$$\underline{u_{nl}}(t) = \underline{u_{switching}}(t) = -(\boldsymbol{S}\cdot\boldsymbol{B})^{-1}\cdot(\left|\boldsymbol{S}\cdot\boldsymbol{B}\right|\cdot\underline{\delta_f} + \underline{\varepsilon_0})\cdot sign(\underline{\sigma_x}(t)) \tag{9}$$

where $\left|\underline{\Delta_x(t)}\right| \le \underline{\delta_f}$ and ε_0 is a positive number [15]. The Lyapunov function has been selected as [15], [16]:

$$\begin{aligned} \underline{V_x}(t) &= \frac{1}{2}\underline{\sigma_x^2}(t) \\ \underline{\dot{V}_x}(t) &= \underline{\sigma_x}(t)\cdot\underline{\dot{\sigma}_x}(t) \end{aligned} \tag{10}$$

From equations (8), (9) and (10), when $t\geq 0$ (with $t_0=0$), there exists a sliding surface $\underline{\sigma_x}(t) = \boldsymbol{S}\cdot\underline{x}(t) = 0$, i.e. $\underline{x}^T(t)\cdot\boldsymbol{S}^T(t) = 0$, the following expressions are obtained:

$$\underline{\dot{\sigma}_x}(t) = -(\left|\boldsymbol{S}\cdot\boldsymbol{B}\right|\cdot\underline{\delta_f} + \underline{\varepsilon_0})\cdot sign(\underline{\sigma_x}(t)) + \boldsymbol{S}\cdot\boldsymbol{B}\cdot\underline{\Delta_x}(t) \tag{11}$$

$$\underline{\dot{V}_x}(t) = -(\left|\boldsymbol{S}\cdot\boldsymbol{B}\right|\cdot\underline{\delta_f} + \underline{\varepsilon_0})\cdot\left|\underline{\sigma_x}(t)\right| + \underline{\sigma_x}(t)\cdot\boldsymbol{S}\cdot\boldsymbol{B}\cdot\underline{\Delta_x}(t) \le -\underline{\varepsilon_0}\cdot\left|\underline{\sigma_x}(t)\right| \tag{12}$$

As proved in [15], [23], the reachability condition is satisfied if $\varepsilon_0 > 0$ and $\Delta_x(t)$ is bounded.

B. Auxiliary feedback and stability analysis

To solve this problem, the sliding mode controller will be designed with a feedback as follows:

$$\underline{u}(t) = -\boldsymbol{K}\cdot\underline{x}(t) + \underline{v}(t) = \underline{u_{eq}}(t) + \underline{u_{nl}}(t) \tag{13}$$

where $\underline{v}(t) = \boldsymbol{K}\cdot\underline{x}(t) + \underline{u_{eq}}(t) + \underline{u_{nl}}(t)$.

$\boldsymbol{K}$ is chosen to get a $\tilde{\boldsymbol{A}} = A + \Delta\boldsymbol{A}(t) - \boldsymbol{BK} = \overline{\boldsymbol{A}} + \Delta\boldsymbol{A}(t)$ stable in closed loop [15], [21]. Selecting the Lyapunov function as $V(t) = x^T(t)Px(t)$ [22], the time derivative of the selected function is:

$$\begin{aligned}\dot{V}(t) &= 2\cdot\underline{x}^T(t)\cdot\boldsymbol{P}\cdot\underline{\dot{x}}(t) = 2\cdot\underline{x}^T(t)\cdot\boldsymbol{P}\cdot(\tilde{\boldsymbol{A}}\cdot\underline{x}(t) + \boldsymbol{B}\cdot(\underline{v}(t) + \underline{\Delta_x}(t)))\\ &= 2\cdot\underline{x}^T(t)\cdot\boldsymbol{P}\cdot\overline{\boldsymbol{A}}\cdot\underline{x}(t) + 2\cdot\underline{x}^T(t)\cdot\boldsymbol{P}\cdot\Delta\boldsymbol{A}\cdot(t)\cdot\underline{x}(t) + 2\cdot\underline{x}^T(t)\cdot\boldsymbol{P}\cdot\boldsymbol{B}\cdot(\underline{v}(t) + \underline{\Delta_x}(t))\\ &= 2\cdot\underline{x}^T(t)\cdot\boldsymbol{P}\cdot(\overline{\boldsymbol{A}} + \Delta\boldsymbol{A}(t))\cdot\underline{x}(t) + 2\cdot\underline{x}^T(t)\cdot\boldsymbol{P}\cdot\boldsymbol{B}\cdot(\underline{v}(t) + \underline{\Delta_x}(t))\end{aligned} \tag{14}$$

For $t \geq t_0$, the sliding variable $\underline{\sigma_x}(t) = \boldsymbol{B}^T\cdot\boldsymbol{P}\cdot\underline{x}(t) = 0$ which implies $2\cdot\underline{x}^T(t)\cdot\mathbf{P}\cdot\mathbf{B}\cdot(\underline{v}(t) + \underline{\Delta_x}(t)) = 0$.

Theorem 1: The uncertain sliding dynamics in (14) is asymptotically stable in closed loop with a state feedback, for Lyapunov function candidate $V(t) = \underline{x}^T(t)\cdot\boldsymbol{P}\cdot\underline{x}(t)$, if there exists a symmetric matrix $P > 0$, satisfying the following LMI:

$$\begin{gathered}(\boldsymbol{A} + \Delta\boldsymbol{A}(t) - \boldsymbol{B}\cdot\boldsymbol{K})\cdot\boldsymbol{Q} + \boldsymbol{Q}\cdot(\boldsymbol{A} + \Delta\boldsymbol{A}(t) - \boldsymbol{B}\cdot\boldsymbol{K})^T + 2\cdot\alpha\cdot\boldsymbol{Q} < 0\\ \boldsymbol{Q} > 0\\ \alpha > 0\end{gathered} \tag{15}$$

with $\boldsymbol{Q} = \boldsymbol{P}^{-1}$. The closed loop system matrix has its eigenvalues strictly on the left hand side of the line α, in complex s-plan.

C. Robust control design

The equation (15) is non-linear matrix inequality, difficult to solve being non convex. It can be solved by increasing α in order to shift the eigenvalues of $\boldsymbol{A}+\Delta\boldsymbol{A}(t)-\boldsymbol{B}\cdot\boldsymbol{K}$ progressively toward the region that guarantees the stability.

However, in order to make the controller more robust against the model uncertainties and non-linearity, we will propose robust design [24], [25].

Consider the uncertain matrix $\Delta\boldsymbol{A}(t)=\boldsymbol{M}\cdot\boldsymbol{\Delta}(t)\cdot\boldsymbol{N}$, where $\boldsymbol{M}$ and $\boldsymbol{N}$ are known, and $\boldsymbol{\Delta}(t)$ is an unknown matrix satisfying $\boldsymbol{\Delta}(t)^T\cdot\boldsymbol{\Delta}(t)\leq I$ [26]. Note that this congruence transformation does not change the definiteness of $\boldsymbol{\Delta}(t)$.

Theorem 2: The uncertain sliding dynamic in (15) can be robustly stabilized if there exists $\boldsymbol{Q}^T>0$, $\boldsymbol{K}>0$ and $\alpha>0$ satisfying the following LMI:

$$\begin{bmatrix} \boldsymbol{A}\cdot\boldsymbol{Q}+\boldsymbol{Q}\cdot\boldsymbol{A}^T-\boldsymbol{B}\cdot\boldsymbol{K}\cdot\boldsymbol{Q}-\boldsymbol{Q}^T\cdot\boldsymbol{K}^T\cdot\boldsymbol{B}^T+2\cdot\alpha\cdot\boldsymbol{Q}+\varepsilon_1\cdot\boldsymbol{M}\cdot\boldsymbol{M}^T & \boldsymbol{N}\cdot\boldsymbol{Q} \\ \boldsymbol{Q}^T\cdot\boldsymbol{N}^T & -\varepsilon_1\cdot\boldsymbol{I} \end{bmatrix}<0 \tag{16}$$

Proof: by replacing $\Delta\boldsymbol{A}$ by $\boldsymbol{M}\cdot\boldsymbol{\Delta}(t)\cdot\boldsymbol{N}$ in (15), it yields

$$\begin{aligned}&\boldsymbol{A}\cdot\boldsymbol{Q}+\boldsymbol{Q}\cdot\boldsymbol{A}^T-\boldsymbol{B}\cdot\boldsymbol{K}\cdot\boldsymbol{Q}-\boldsymbol{Q}\cdot\boldsymbol{B}\cdot\boldsymbol{K}+2\cdot\alpha\cdot\boldsymbol{Q}+\boldsymbol{M}\cdot\boldsymbol{\Delta(t)}\cdot\boldsymbol{NQ}\\&+\boldsymbol{Q}^T\cdot\boldsymbol{N}^T\cdot\boldsymbol{\Delta(t)}\cdot\boldsymbol{M}^T<0\end{aligned} \tag{17}$$

with the assumption $\boldsymbol{\Delta}(t)^T\boldsymbol{\Delta}(t)\leq I\rightarrow\|\boldsymbol{\Delta}(t)\|<I$, as given in [25] and [26], it follows that:

$$\boldsymbol{M}\cdot\boldsymbol{\Delta}(t)\cdot\boldsymbol{N}\cdot\boldsymbol{Q}+\boldsymbol{Q}^T\cdot\boldsymbol{N}^T\cdot\boldsymbol{\Delta}(t)\cdot\boldsymbol{M}^T\leq\varepsilon_1^{-1}\cdot\boldsymbol{M}\cdot\boldsymbol{M}^T+\varepsilon_1\cdot\boldsymbol{N}\cdot\boldsymbol{Q}\cdot\boldsymbol{Q}^T\cdot\boldsymbol{N}^T \tag{18}$$

with $\varepsilon_1>0$, the inequality (17) is satisfied if the following equation is satisfied:

$$\begin{aligned}&\boldsymbol{A}\cdot\boldsymbol{Q}+\boldsymbol{Q}\cdot\boldsymbol{A}^T-\boldsymbol{B}\cdot\boldsymbol{K}\cdot\boldsymbol{Q}-\boldsymbol{Q}\cdot\boldsymbol{B}\cdot\boldsymbol{K}+2\cdot\alpha\cdot\boldsymbol{Q}+\varepsilon_1^{-1}\cdot\boldsymbol{M}\cdot\boldsymbol{M}^T\\&+\varepsilon_1\cdot\boldsymbol{N}\cdot\boldsymbol{Q}\cdot\boldsymbol{Q}^T\cdot\boldsymbol{N}^T<0\end{aligned} \tag{19}$$

Using Schur complement, we can put (19) in the form (16) as desired. The proposed robust Sliding Mode Controller (SMC) can be constructed similar to the previous algorithm by replacing (15) by (16) [27].

D. Chattering reduction

The sliding mode control law of (13), with LMI constraints (19) guarantees the asymptotic stability of $x(t)=0$ in error coordinates, eliminating the effect of uncertainties and perturbations on system state variables. In order to restrain the chattering phenomena, a continuous function $\underline{k}\cdot\underline{\sigma_x}(t)$ can be chosen instead of discontinuous function $sign(\underline{\sigma_x}(t))$ [23], [28], [29]. The nonlinear part of the controller can be expressed as:

$$\underline{u_{nl}}(t) = -(\boldsymbol{S}\cdot\boldsymbol{B})^{-1}\cdot(|\boldsymbol{S}\cdot\boldsymbol{B}|\cdot\underline{\delta_f}+\underline{\varepsilon_0})\underline{\cdot k}\cdot\underline{\sigma_x}(t) \tag{20}$$

with $k > 0$.

4. GA/PSO robust design approach

From theoretical point of view, the proposed controller can be considered as an optimization of a robust sliding mode controller. The optimization of the controller parameter has a vital role in the design of such a sliding mode controller. A properly optimized controller tries to minimize an appropriate objective function of the system and it assures the process output to track the desired target as well as to reduce the effect of perturbations affecting the system. To optimize a sliding mode controller, there is not any method that has been specified in the literature survey [30]. In the present work, GA and PSO are used to optimize the controller parameters.

A. The proposed Algorithm

The steps involved in the proposed GA/PSO Robust sliding mode control algorithm are:

Phase A (previous sections) - Robust sliding mode control:

Step1: Design of the dynamic control based on equivalent and switching control, as illustrated in equations (8) and (9).
Step2: Ensure the asymptotic stability of the proposed controller, as illustrated in equations (12) and (14).
Step3: After designing the robust sliding surface, the system dynamic will be driven onto the sliding surface, and remain on it. The resulting problem in (14) can be transformed to Linear Matrix Inequality (LMI) optimization in equation (16). These resulting optimization problems can be solved numerically very efficiently using developed interior-point methods implemented in MATLAB software.

Phase B (current Section) - Optimization of robust sliding mode control:

Step4: In the conventional robust sling mode control, it is primordial to have the information about the uncertainties, in order to design a control law with switching part dominating the effect of perturbations [29]. To overcome this, in this section we propose to optimize the parameters of robust sliding mode control using Genetic Algorithm (GA) and Particle Swarm Optimization (PSO) based on using equations (12) and (20), and on the block diagram in *Fig. 2*.

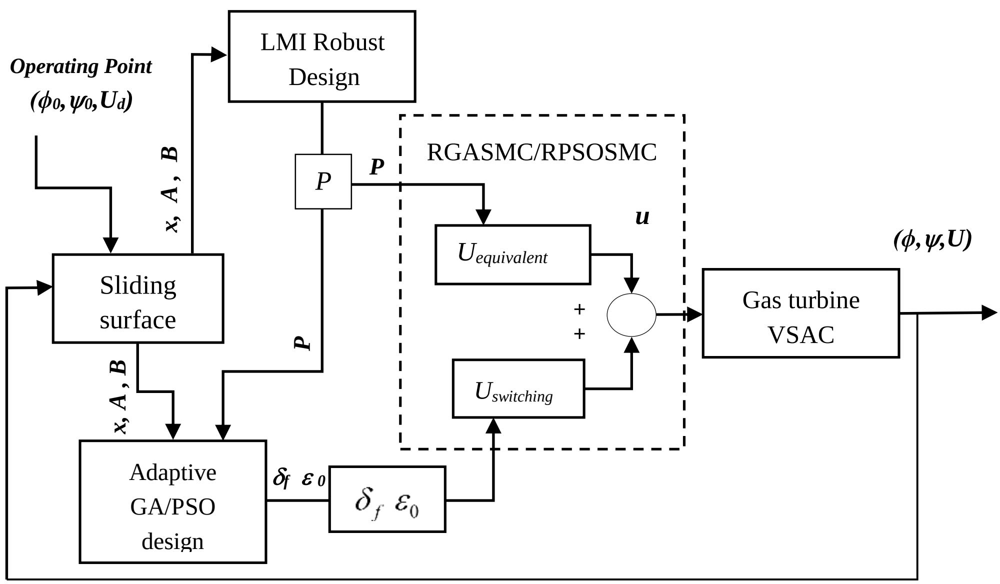

Figure 2: The block diagram of proposed control.

The objective function comprises robust performance and stability criterion which is required to optimize the use of switching control efforts. The objective function is given by equation (21).

$$
\begin{aligned}
&\min \quad f(\underline{\delta_f},\underline{\varepsilon_0},\underline{k}) = \underline{u}(\underline{\delta_f},\underline{\varepsilon_0},\underline{k})^T \cdot \underline{u}(\underline{\delta_f},\underline{\varepsilon_0},\underline{k}) \\
&\textit{Subjected to} -(|\mathbf{S}\cdot\mathbf{B}|\cdot\underline{\delta_f}+\underline{\varepsilon_0})\cdot\underline{k}\cdot\underline{\sigma_x}^2(t)+\sigma_x(t)\cdot\mathbf{S}\cdot\mathbf{B}\cdot\underline{\Delta_x}(t)<0\cdots(a) \\
&u_2>0\cdots\cdots\cdots\cdots\cdots\cdots\cdots\cdots\cdots\cdots(b) \\
&\underline{\delta_f}>0\cdots\cdots\cdots\cdots\cdots\cdots\cdots\cdots\cdots\cdots(c) \\
&\underline{\varepsilon_0}>0\cdots\cdots\cdots\cdots\cdots\cdots\cdots\cdots\cdots\cdots(d)
\end{aligned}
\tag{21}
$$

In equation (21), the constraint (a) is required to generate a robust stability bound for the given model specifications and amount of plant uncertainties by using compressor map curve and throttle dynamic. The reachability condition (a) is a feasible optimization $-(|\boldsymbol{S}\cdot\boldsymbol{B}|\cdot\underline{\delta_f}+\underline{\varepsilon_0})\cdot\underline{k}\cdot\underline{\sigma_x}^2(t)+\underline{\sigma_x}(t)\cdot\boldsymbol{S}\cdot\boldsymbol{B}\cdot\underline{\Delta_x}(t)\le-\underline{\varepsilon_0}\underline{k}\underline{\sigma_x}^2(t)$, for $\underline{\varepsilon_0}>0$ and $\underline{k}\underline{\sigma_x}^2(t)$ is a positive definite function [15], [19]. Then, with the flexibility of the GA and PSO algorithms, these numerical bounds can be used directly in an online optimization of decision variables δ_f , ε_0 and k is a positive constant as an adaptive gain.

B. Genetic Algorithm Optimization (GA)

The genetic algorithm is a heuristic approach to solving a non-linear optimization problem, which is essentially based on the theory of natural selection, the process that drives biological evolution [31]. In all global search problem, there is an optimization problem of maximizing or minimizing an objective function for a given space of arbitrary dimension [32-34]. In this paper the objective function is the equation (21), where δ_f, ε_0 are decision variables. The flowchart in *Fig. 3* explains the process in brief. The implementation of the GA is based on the following fundamental initializations: chromosome representation, selection function, the genetic operators, initialization, termination and evaluation function. A variety of constraints-handling methods for genetic algorithms have been developed in the last decades. Most of them can be classified into two main types of concepts: penalty function and multi-objective optimization concept [34], [35]. In this work, the used concept to constraints-handling is the penalty function.

C. Particle Swarm Optimization (PSO)

Particle Swarm Optimization (PSO) is a derivative-free global optimum solver. It is inspired by the surprisingly organized behavior of large groups of simple animals, such as flocks of birds, schools of fish, or swarms of locusts [36]. The nonlinear optimization is illustrated in equation (21), where δ_f, ε_0 are decision variables. The flowchart in *Fig. 4* explains the process in brief. The individual creatures, or “particles”, in this algorithm are primitive, knowing only four simple things, their own current location in the search space and fitness value, their previous personal best location, and the overall best location found by all the particles in the “swarm”. There are no gradients or Hessians to calculate. Each particle continually adjusts its speed and trajectory in the search space based on this information, moving closer towards the global optimum with each iteration. As seen in nature, this computational swarm displays a remarkable level of coherence and coordination despite the simplicity of its individual particles. While the particles in the PSO algorithm are searching the space, each particle remembers two positions. The first is the position of the best point the particle has found (self- best), while the second is the position of the best point found among all particles (group-best). Let *X* and *V* represent the particle position and velocities in the given search space, respectively. Therefore, the i-th particle is represented as $X_i = (x_{i1}, \ldots\ldots.. x_{im})$, in the m-di-mensional search space. The previous position of the i-th particle is recorded and represented as $j_{p\,best} = (j_{p\,best_{t1}}, \ldots\ldots. j_{p\,best_{tm}})$. The index of the best particle among all the particles in the group is represented by j_{pbest}. The rate of the velocity for particle i is represented as $V_i = (v_{i1}, \ldots\ldots.. v_{in})$. The modified velocity and position of each particle can be calculated using the current velocity and distance from J_{pbest} and J_{gbest} use the following equations:

$$\underline{V_i^{t+1}} = Q_p \cdot \underline{V_i^t} + K_1 \cdot rand_1 \cdot (\underline{X_{pbest}} - \underline{X_i^t}) + K_2 \cdot rand_2 \cdot (\underline{X_{gbest}} - \underline{X_i^t}) \tag{22}$$

$$\underline{X_i^{t+1}} = \underline{X_i^t} + \gamma \cdot \underline{V_i^{t+1}} \tag{23}$$

Where K_1 and K_2 are two positive constants, $rand_1$ and $rand_2$ are random numbers in the range [0,1], and Q_p is the inertia weight. X_i^t represents the current position of the i-th particle and V_i^t is its current velocity. The positions of the particles are updated using Equation (23), where X_i^{t+1} is the new position of the i-th particle of m-dimensional search space, where "*iter*" is the iteration count [37]. Particle swarm optimization is guided by the quality of its candidate solutions. Consequently, an obvious solution to constraint handling is to penalize the fitness of infeasible methods. Penalty method (penalty functions) is easy to implement, and shows an improvement of the approximation of optima with active constraints [36], [38]. The weight Q_p is updated using the following equation:

$$Q_p = Q_{p\max} - \left[\frac{Q_{p\max} - Q_{p\min}}{iter_{\max c}} \right] \cdot iter \tag{24}$$

The parameters used for GA and PSO performed in the present study are given in *Table 1* and *Table 2*.

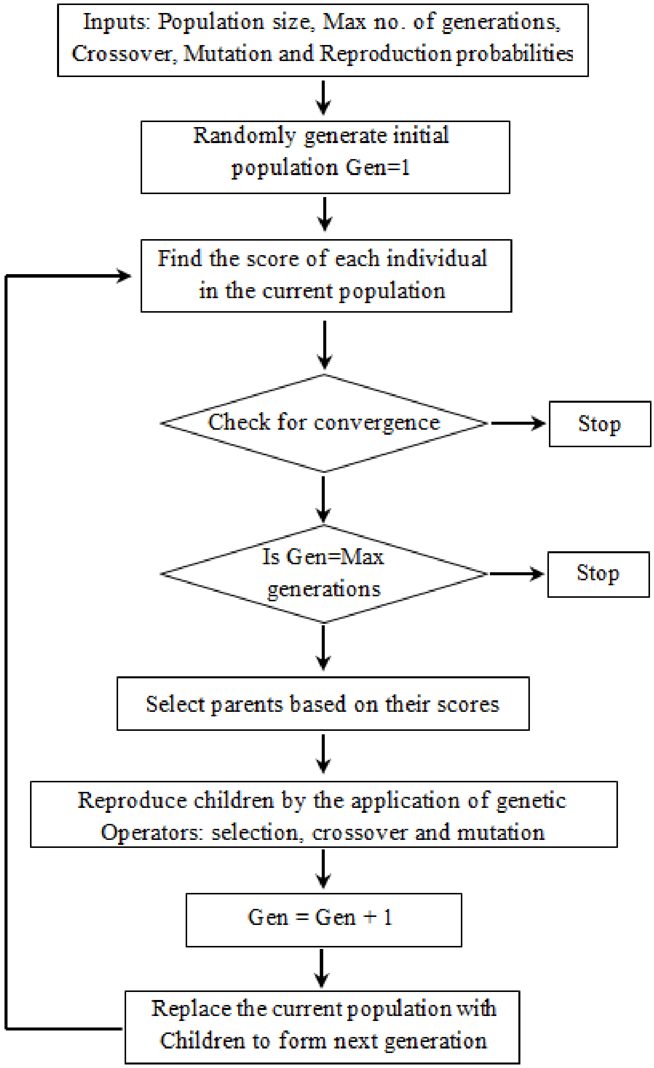

Figure 3: Flowchart of Genetic Algorithm Optimization (GA).

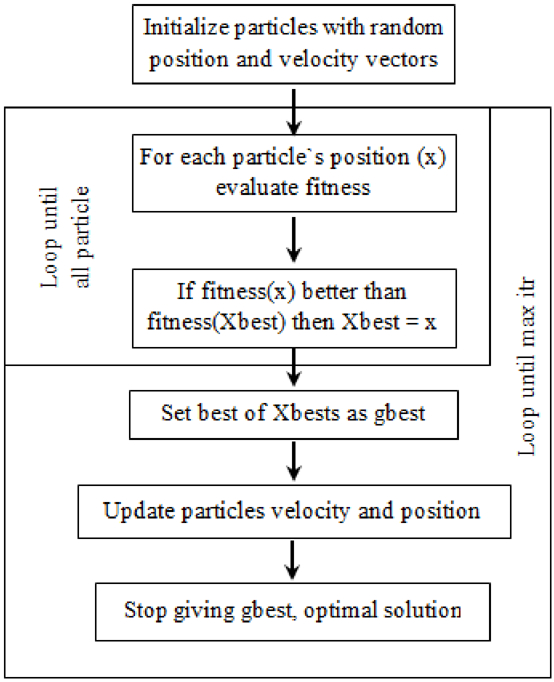

Figure 4: Flowchart of Particle Swarm Optimization (PSO).

Table 1: GA Parameters used in the simulation

Parameter	Value
Population size	40
Maximum number of generations	50
Type of selection	Roulette wheel
Type of crossover	Intermediate
Fitness function	Equation (21)
Constraints-handling methods	Penalty function
Type of mutation	adapt feasible
Crossover Ration	0.8

Table 2: PSO Parameters used in the simulation

Parameter	Value
Maximum iteration	50
Population size	40
Dimension	2
Value of K2	2.0
Maximum weight	0.90
Minimum weight	0.40
Fitness function	Equation (21)

5. Numerical simulation

For simulation purposes it is considered the compressor model of Gravdahl as given in equations (1) to (5), with numerical values are given in *Table 3* [2], [5].

Table 3: Model parameters used in simulation

Parameter	Value	Parameter	Value	Parameter	Value	Parameter	Value
W	0.25	a	0.3	b	96.16	d_Ψ	0.02
H	0.18	l_i	1.75	m	1.75	Λ_1	$2.168e\text{-}4$
μ	0.01	d_Φ	-0.05	l_E	3	Λ_2	0.0189
ρ_1	$0<\rho_1<1$	ρ_2	$0<\rho_2<1$	c	0.7	γ_v	1

The aim of this simulation is demonstrating the effectiveness and the robustness of the proposed controllers in preventing the compressor from developing temporary rotating stall ($J_1>0$), and pressure drop under the following critical operating conditions:

1- Constrained Throttle valve opening ($u_2>0$): It is interesting to note that in [2], [4], [5], [14] it is reported that the saturated effort of the throttle valves can cause a temporary rotating stall.

2- Speed Transition: As reported in [2], [4], [5], [14], when speed varies at an efficient operating point (0.5,0.66) temporary stall developments can lead to a fully developed rotating stall.

3-Pertubations: Previously reported results in [1], [2], [5] show that pressure and flow external perturbations can destroy the stability of compressors at an efficient operating point (0.5, 0.66) and lead to fully developed rotating stall or deep surge depending on the speed of the rotor (i.e. for low speeds the system goes to rotating stall and for high speeds it develops deep surge). Two types of perturbations are applied to the system denoted by $\Phi_d(t)=\Psi_d(t)=0.01\sin(0.2t)$, they are considered as mass flow and pressure disturbances respectively and, d_Φ, d_Ψ represent the uncertainty of the compressor map and throttle characteristic. At $t=1000$ a higher perturbation magnitude $\Phi_d(t)=\Psi_d(t)=0.1\sin(0.2t)$ is applied to system to check the robust and adaptive behaviour of the three proposed controllers. The simulation numerical values are given in *Table 3* [2], [5].

In **TEST 1**, perturbations are applied and constrains are considered. A low desired speed $U_d = 40\ m/s$ of the turbine is considered. In **TEST 2**, perturbations are applied and constrains are considered. A high desired speed $U_d = 150\ m/s$ of the turbine is considered. In order to illustrate the advantage of the proposed robust sliding mode controller without optimization **(RSMC)**, Genetic Algorithm optimized robust sliding mode controller **(RGASMC)**, and particle swarm optimized robust sliding mode controller **(RPSOSMC)** a comparative simulation is carried out using Matlab software.

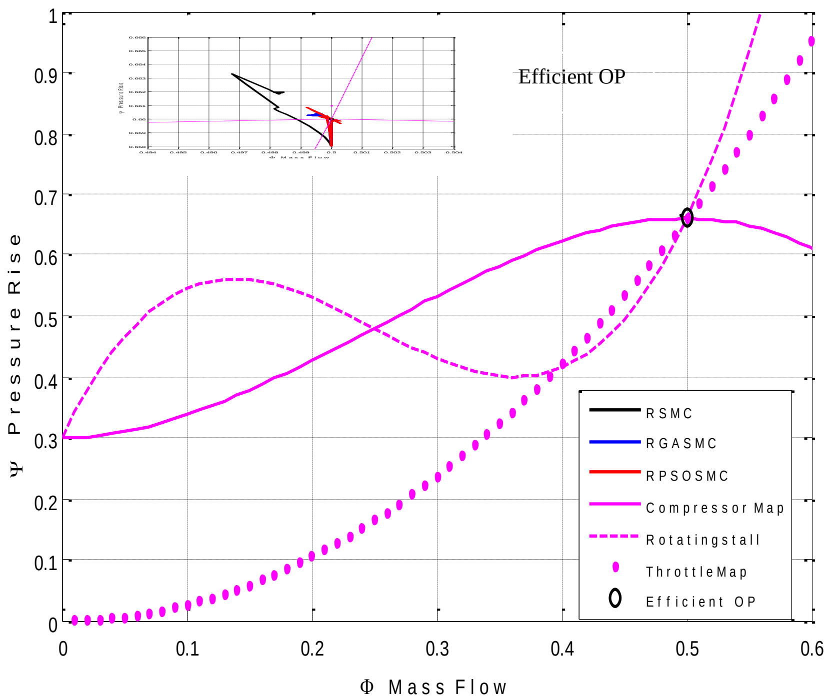

Figure 5: Closed loop system map ***TEST1.***

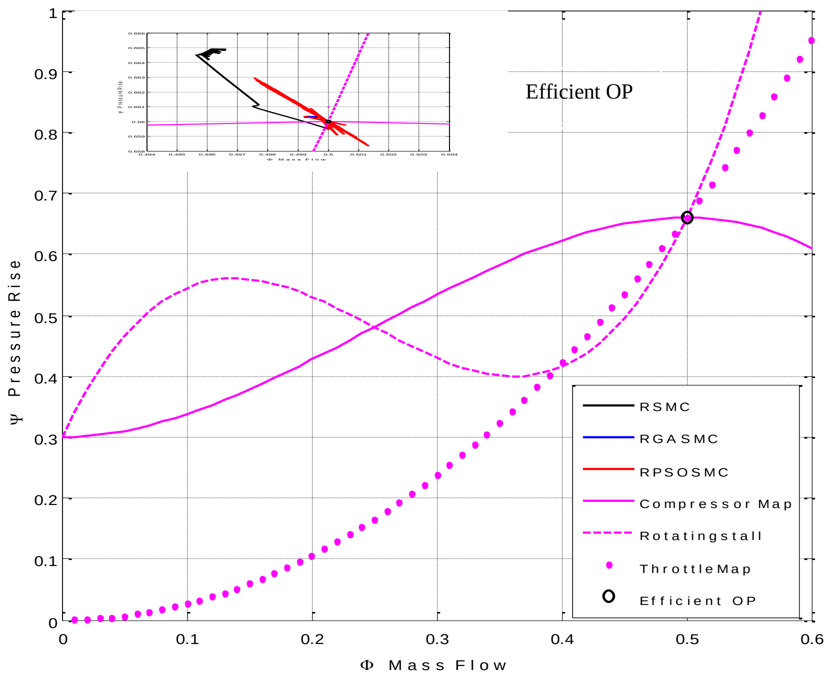

Figure 6: Closed loop system map ***TEST 2.***

For the tests **TEST1** and **TEST2**, *Fig. 5* and *Fig. 6* show the variables Φ and Ψ in the phase space along with compressor map and stall characteristic. The system starts from an effective initial operating point (OP) at the top of the compressor map. At *t=0*, the controller is activated and closes the loop. Examining *Fig.* 5 and *Fig. 6*, we found that, the proposed controllers effectively stabilize the compression system at the efficient point OP and prevent it from developing a steady rotating stall due to the speed variation, thus limiting the throttle valve opening coefficient which must always be positive·

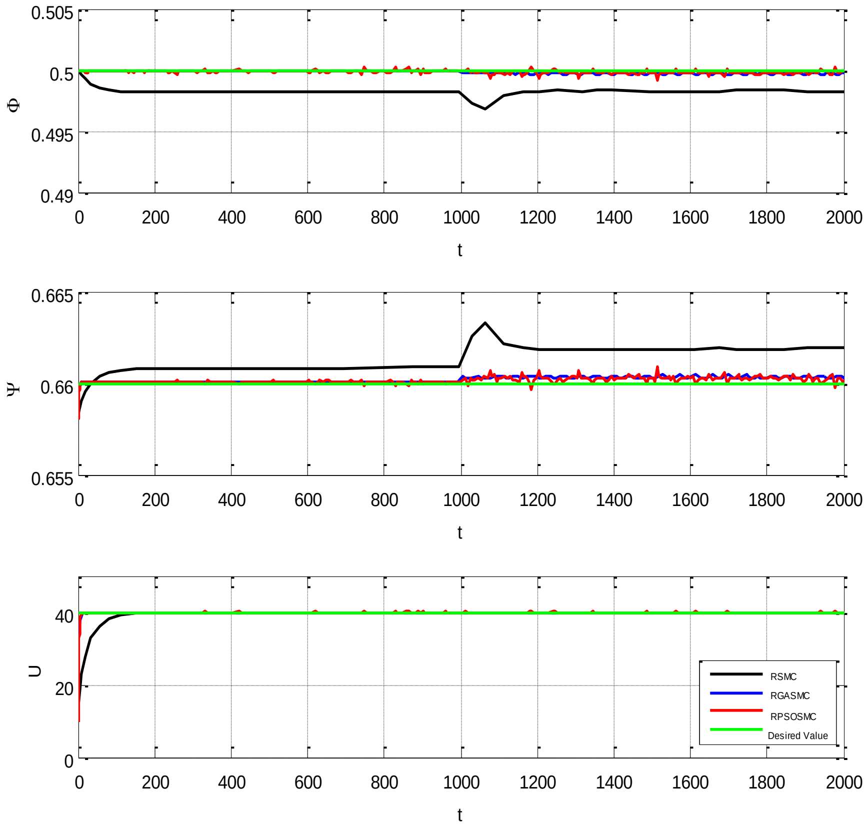

Figure 7: Output dynamic in closed loop ***TEST 1.***

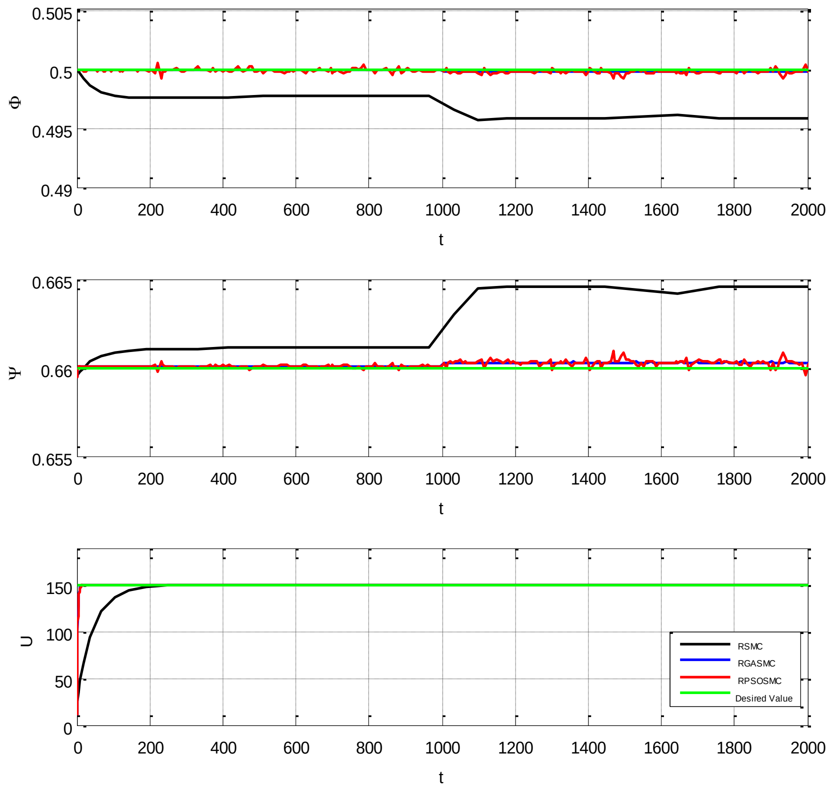

Figure 8: Output dynamic in closed loop ***TEST 2.***

In *Fig. 7* and *Fig. 8*, we found that the RGASMC and RPSOSMC controllers make the compressor operating close to his efficient OP *(Φ,Ψ)=(0.5,0.66)* despite the existence of uncertainties, and perturbation (negligible variation). The robust sliding mode controller (RSMC) can't reject the effect of the perturbation. This can be explained by the need of the prior knowledge of the upper bound of the perturbations and uncertainties, governed by $|\Delta_x|\leq\delta_f$. Compared to (RSMC) and many control strategies proposed in the previous literature, one advantage of the proposed GA and PSO controllers designed in this paper is their ability to be applied in real applications without a need to a prior knowledge on perturbations and uncertainties.

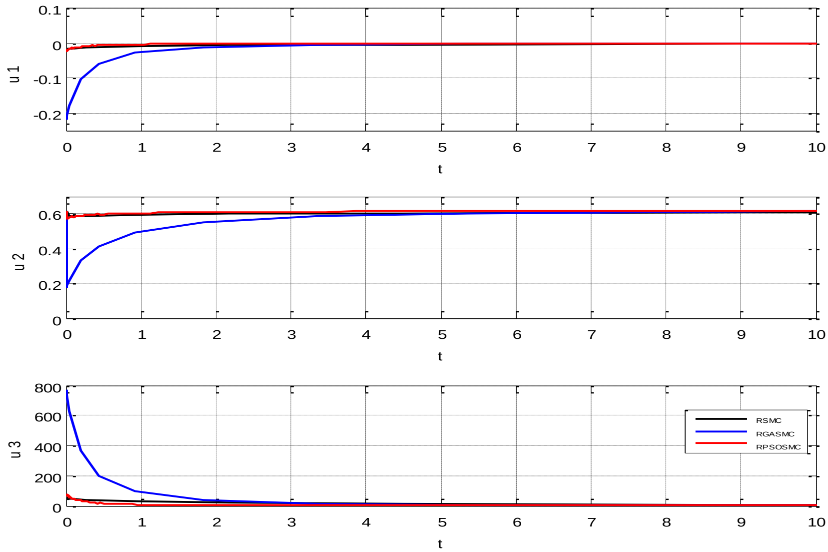

Figure 9: Control efforts dynamic in closed loop ***TEST 1.***

In *Fig. 9* and *Fig. 10*, we have noted a variation in throttle actuator, despite that the system still reaches its stable OP, where the pressure is high enough for normal operation of the gas turbine.

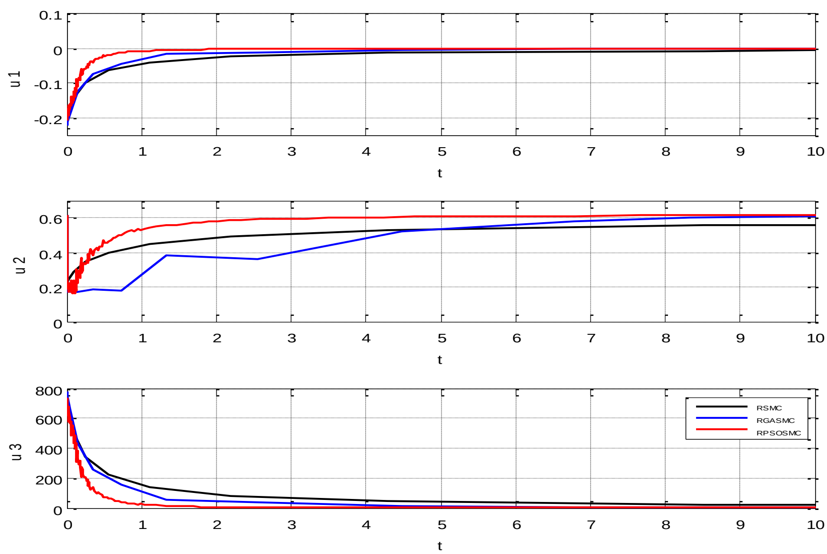

Figure 10: Control efforts' dynamic in closed loop ***TEST 2.***

The throttle gain decrease is caused by the high level of perturbation on the pressure rate, which is a consequence of the low speed of the turbine during the starting phase (9.617 m/s). The throttle valve immediately damps out rotating stall as illustrated in [10], it should be turned down in order to add some resistance to the compression system when the flow change is positive and the pressure change rises is not negative. It can be seen that the throttle gain for the three controllers is still positive and lower than one $0 < u_2 < 1$.

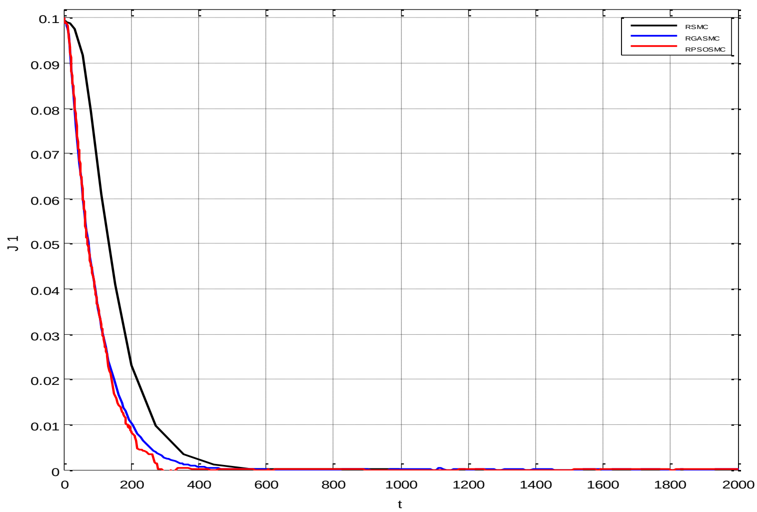

Figure 11: The first harmonic of rotating stall ***TEST 1.***

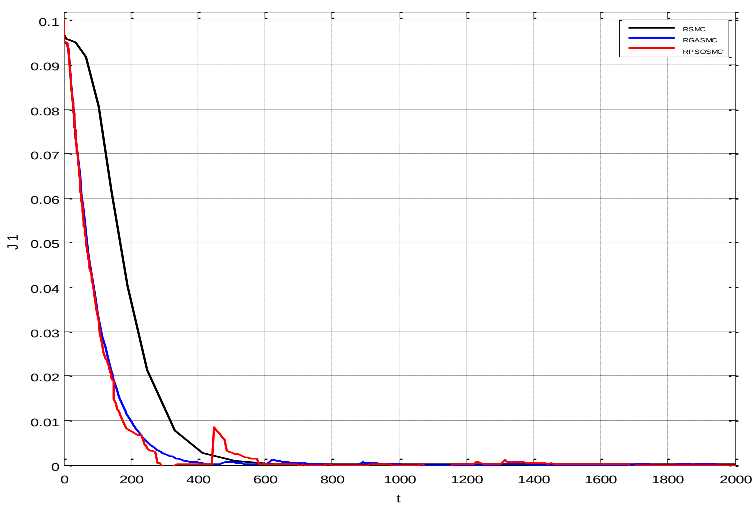

Figure 12: The first harmonic of rotating stall ***TEST 2.***

Fig. 11 and *Fig. 12* show the effectiveness of the proposed control law regarding the rotating stall control. It can be noticed that, even though the cumulative computational time increases linearly with the number of generations for both PSO and GA, the computational time for GA is low compared to the PSO optimization algorithm.

6. Conclusion

This paper has presented a GA and PSO adaptive sliding mode controller design based on linear matrix inequality. The proposed approach is applied to the gas turbine, which is a variable speed system, by its nature. This turbine suffers from temporarily developed instabilities which may lead to a steady and fully developed rotating stall or surge. The used model reveals significantly the impact of speed transitions (measurable output) and throttle gain (control effort) on the stability of the compression system. The addition of model uncertainties and external perturbations and impossibility to have a full feedback control (rotating stall is not measurable) constitute a challenging issue. The proposed controllers do not require precise knowledge of the compressor map, an upper bound of the uncertainties and perturbations, and do not use a full-state feedback. Time-domain simulations have demonstrated that RGASMC and RPSOSMC controllers are still stable, close to desired performances and are damping out system instabilities including surge and rotating stall.

Appendix: Nomenclature of the model variables:

ϕ: Annulus averaged mass flow coefficient

ψ : Plenum pressure rise coefficient

J_1: The first mode squared amplitude of rotating stall

U : Rotor tangential velocity at mean radius

U_d : Desired constant velocity

γ_T : Throttle Gain

γ_v : Close Coupled valve gain

t : Non-dimensional time

t_d : Dimensional time

U_0 : compressor initial velocity

$d_\phi, d\psi$: Mass flow and pressure uncertainty

Φ_d, Ψ_d : Time varying and mass flow pressure disturbance

R : mean compressor radius

$\Psi_c(\Phi)$: Compressor characteristic

$\Psi_s(\Phi)$: Stall characteristic

H : semi-height of the compressor characteristic

W : semi-width of the compressor characteristic

ψ_{c0} : shut-off value of the compressor characteristic

l_c, l_i, l_E : Effective flow passage non-dimensional length of the compressor, Inlet duct and exit duct respectively.
m : Compressor duct flow parameter
c: Coefficient of compressor torque.
a : Reciprocal time lag parameter of the blade passage
a_s : Sonic velocity
μ : Viscosity
Λ_1, Λ_2 : Constants in Greitzer model
b : Constant in Greitzer model

References

[1] Gravdahl, J. T., and Egeland, O., "Moore-Greitzer Axial Compressor Model with Spool Dynamics", in *Proc. of 36th IEEE Conference on Decision and Control*, 1997, pp. 4714–4719.

[2] Gravdahl, J. T., and Egeland,O., "Compressor surge and rotating stall Modelling and control", Advances in Industrial Control. Springer Verlag. London Limited, 1999.

[3] Sari, G., Akhrif, O., and Saydy, L., "Qualitative Analysis of an Axial Compressor Model with Non-constant Speed", in *Proc. of ASME 2011 Power Conference*, Vol. 1, 2011, pp. 515–524.

[4] Sari, G., Akhrif, O., and Saydy, L., "The impact of speed variation on the stability of variable speed axial compressors at efficient operating points", in *Proc. of American Control Conference*, 2012, pp. 404–410.

[5] Sari.O., "Model analysis and nonlinear control of air compressors", *PhD thesis*. Montreal University, 2014.

[6] Sheng, H., Huang, W., Zhang, T., and Huang, X., "Robust Adaptive Fuzzy Control of Compressor Surge Using Back-stepping", *Arabian Journal for science and engineering*, Vol. 39, Issue.2, pp. 9301–9308, December 2014.

[7] Moghaddam, J. J., and Madani, M., "A decoupled adaptive neuro-fuzzy sliding mode control system to control rotating stall and surge in axial compressors", *Journal of Expert Systems with Applications*, Vol. 38, Issue. 4, pp. 4490–4496, April 2011.

[8] Zaiet, C., Akhrif, O., and Saydy, L., "Modeling and Non Linear Control of a Gas Turbine", International Symposium on Industrial Electronics ISIE 2006, 2006, pp. 2688–2694.

[9] Fontaine, D., Liao, S., Paduano, J., and Kokotovic, P., "Nonlinear control experiments for rotating on an axial flow compressor", in *Proc. of 39th IEEE conference on decision and control*, 2000, pp. 1329–1334.

[10] Lin, S., Yang, C., Wu, P., and Song, Z., "Fuzzy logic surge control in variable speed axial compressors", in *Proc. of 10th IEEE International Conference on Control and Automation* (*ICCA*), 2013, pp. 1178–1183.

[11] Uddin, N., and Gravdahl, J.T., "Active compressor surge control using piston actuation", in *Proc. ASME 2011 Dynamic Systems and Control Conference DSCC2011*, 2011, pp. 69–76.

[12] Moghaddam, J. J., Farahani, M. H., and Amanifard, N., "A neural network-based sliding-mode control for rotating stall and surge in axial compressors", *Journal of Applied Soft Computing*, Vol.11, Issue. 1, pp. 1036–1043, January 2011.

[13] Sheng, H., Huang, W., and Zhang, T., "Output feedback control of surge and rotating stall in axial compressors", *Asian Journal of Control*, Vol. 19, Issue 1, pp.1–7, September 2016.

[14] Debbah, A., Kharfene, H., Karboua, A., "Using Robust sliding mode controller to improving the aerodynamic performance of a gas turbine", in *Proc. of the 4th International Seminar on New and Renewable Energies*, 2016, pp. 1–6.

[15] Lui, J., "Advanced sliding mode control for mechanical systems". Springer. Tsinghua University Press. Beijing, 2012.

[16] Defoort, M., Floquet, T., Kokosy, A., and Perruquetti, W., "A novel higher order sliding mode control scheme", *Journal of Systems and Control Letters Elsevier*, Vol. 58, Issue. 2, pp. 102–108, 2009.

[17] Tsai, C., and Wu, H., "Robust passivity-based control of weakly minimum phase nonlinear uncertain systems: An application to manipulator", in *Proc. of 7th Asian Control Conference,* ASCC, 2009, pp. 919–924.

[18] Feher, A., Kutasi, D. N., "Modelling and control of bounded hybrid systems in power electronics*", Acta Universitatis Sapientiae, Electrical and Mechanical Engineering*, Vol. 9, Issue 1, pp. 33–42, December 2017.

[19] Horvath,Z., Edelmayer, A., "Robust model-based detection of faults in the air path diesel engines ", *Acta Universitatis Sapientiae, Electrical and Mechanical Engineering*, Vol. 7, Issue 1, pp. 5–22, December 2015.

[20] Fodor, D., "Experimental investigation on robust control of induction motor using H_∞ output feedback*", Acta Universitatis Sapientiae, Electrical and Mechanical Engineering*, Vol. 1, Issue 1, pp. 29–40, December 2009.

[21] Chen, P.V., Chiang, C. H., and Liu, J. C., "The input/output constrained control for V/STOL aircraft dynamics under a descriptor system formulation", *Journal of Aeronautic and aviation*, Vol. 41, Issue 1, pp. 43–52, January 2009.

[22] Kelemen, A., Kutasi, N., "Lyapunov-based frequency-shift power control of induction-heating converters with hybrid resonant load", *Acta Universitatis Sapientiae, Electrical and Mechanical Engineering*, Vol. 1, Issue 1, pp. 41–52, December 2009.

[23] Leu,V. Q., Choi, H. H., and Jung, J. H., "LMI based sliding mode speed tracking control design for surface-mounted permanent magnet synchronous Motors", *Journal of Electrical Engineering and Technology*, Vol. 7, Issue 4, pp. 513–523, July 2012.

[24] Der-Cherng, L., Ren, S. M., and Shih-Tse, S., "A Feedback Linearization Design for Compressor's Surge Control", in *Proc. of Industrial Technology ICIT*, 2008, pp. 1–6.

[25] Boyd, S., El Ghaoui, L., Feron, E., and Balakrishnan, V., "Linear Matrix Inequalities in System and Control Theory", SIAM. Philadelphia, 1994.

[26] Argha, A., Li, L., SU, S. H., and Nguyen, H., "A new LMI-Based Robust Sliding Mode control for the uncertain Discrete-Time system", in *Proc. of 53th IEEE Conference on Decision and Control*, 2014, pp. 4747–4752.

[27] Mahmoud, M. S., and Soliman, H. M., "Design of Robust Power System Stabilizer Based on Particle Swarm Optimization", *Journal of Circuits and Systems*, Vol. 3, pp. 82–89, 2012.

[28] Chen, D.Y., Liu, Y. X., Ma, X. Y., and Zhang, R. F., "No-chattering sliding mode control in a class of fractional-order chaotic systems", *Chinese Physics B*, Vol. 2, No. 20, pp. 120506-1–120506-9, December 2011.

[29] Hu, X., Wu, L., Hu, C., and Gao, H., "Adaptive sliding mode tracking control for a flexible air-breathing hypersonic vehicle", *Journal of the Franklin Institute*, Vol. 349, Issue. 2, pp. 559–577, Marsh 2012.

[30] Kumar, J., Azar, A. T., Kumar. V., and Rana K. P. S., "Design of Fractional Order Fuzzy Sliding Mode Controller for Nonlinear Complex Systems", Chapter 9, Advances in Nonlinear Dynamics and Chaos (ANDC) Elsevier, pp. 249–282, 2018.

[31] Panda, S., and Padhy, N, P., "Comparison of particle swarm optimization and genetic algorithm for FACTS-based controller design", *Elsevier Applied Soft Computing*, Vol. 8, Issue. 4, pp. 1418–1427, September 2008.

[32] Laminia, C., Benhlimab, S., and Elbekria, A., "Genetic Algorithm Based Approach for Autonomous Mobile Robot Path Planning", *Journal of Procedia Computer Science Elsevier*, Vol. 127, pp. 180–189, 2018.

[33] Khan, A. A., and Mir, R. N., "Optimization of Constrained Function Using Genetic Algorithm", *Journal of Computer Engineering and Intelligent System*, Vol. 8, No. 2, pp. 11–15, 2017.

[34] Deb, K., "An Efficient Constraint Handling Method for Genetic Algorithm. Computer Methods in Applied Mechanics and Engineering", *Journal of Computer Methods in Applied Mechanics and Engineering Elsevier*, Vol. 186, Issue 2–4, pp. 311–338, June 2000.

[35] Kramer, O., "A Review of Constraint-Handling Techniques for Evolution Strategies", *Journal of Applied Computational Intelligence and Soft Computing*, Vol. 2010, pp. 1–11, January 2010.

[36] Yanzhi, R., and Sanyang, L., "Modified particle swarm optimization algorithm for engineering structural optimization problem", in *Proc. of 13th International Conference on Computational Intelligence and Security*, 2017, pp. 504–507.

[37] Satpati, B., Koley,C., and Datta, S., "Robust PID controller design using particle swarm optimization-enabled automated quantitative feedback theory approach for a first-order lag system with minimal dead time", *Journal of Systems Science & Control Engineering*, Vol. 2, Issue 1, pp. 502–511, April 2014.

[38] Juneja, M., and Nagar, S.K., "Particle swarm optimization algorithm and its parameters: A review", *in Proc. of International Conference on Control. Computing Communication and Materials (ICCCCM)*, 2016, pp. 1–5.